An Approach to Reconstruction of a Natural Crack using Signals of Eddy Current Testing I. Reconstruction of an Idealized Natural Crack

December 1998

O-arai Engineering Center
Japan Nuclear Cycle Development Institute

JNC TN9400 99-009
December, 1998

An Approach to Reconstruction of a Natural Crack using Signals of Eddy Current Testing

I. Reconstruction of an Idealized Natural Crack

Zhenmao CHEN*

Abstract

In this paper, an approach to the reconstruction of an idealized natural crack of non-vanishing conductivity is proposed with use of signals of eddy current testing. Two numerical models are introduced at first for modeling a Stress Corrosion Crack (SCC) in order it possibly to be represented by a set of crack parameters. A method for rapid prediction of the eddy current testing signals arisen from these idealized cracks is given then by extending a knowledge based fast forward solver developed by authors to the case of a non-vanishing conductivity. On the other hand, the inverse algorithm of conjugate gradient method is improved to reconstruct the crack parameters and is implemented with the pick-up signals and gradients calculated by using the rapid forward solver. Several examples are presented finally for validating the proposed strategy. The results verified that both of the models can give reasonable reconstruction results in case of a low noise level. The model concerning the touch of crack surfaces with a conducting band region surrounded by the crack edge, however, is proved more efficient than the model using a conductivity distribution from the point of view of both reconstruction speed and accuracy.

---

* Doctoral Fellow, Structure Safety Engineering Group, OEC/JNC
4002 Narida, Oarai, Ibaraki, 311-1393, Japan.

JNC TN9400 99-009
１９９８年12月

渦電流探傷法結果に基づく自然き裂の再構成 その１ 接触のある理想き裂の場合

陳 振茂*

要旨

本報告書では、渦電流探傷信号に基づいて接触のあるき裂の再構成手法を提案・検証した。まず、自然き裂を離散化するために２種類のき裂モデルを提案し、それに基づいてき裂によるECT信号及びその勾配を高速且つ高精度的に計算する手法を開発した。更に上記順問題の高速ソロバー及びモデル化した自然き裂に基づき、最適化手法の共役勾配法を改良し、異なる種類のき裂パラメータを同時に逆推定することに成功した。具体的に矩形き裂に対して再構成を行った結果、２種類のき裂モデル共に接触のあるき裂の再構成に有効であることを実証した。但し、接触がき裂の境界部に限った２番目のモデルはより効率よく再構成することができると判った。本研究の結果は、表面き裂の非破壊検査技術の向上に貢献することが期待できる。

* 大洗工学センター、Na安全工学試験部、機器・構造安全工学グループ、博士研究員

Contents

List of Abbreviations

BEM	Boundary Element Method
CG	Conjugate Gradient
ECT	Eddy Current Testing
EDM	Electro-Discharge Machining
FEM	Finite Element Method
ID	Inner Defect
IGA	InterGranulur Attack
ISI	In-Service Inspection
NDE	Non-Destructive Evaluation
NDT	Non-Destructive Testing
PWR	Pressurized Water Reactor
SCC	Stress Corrosion Crack
SG	Steam Generator

List of Notations

$\boldsymbol{A}$	Magnetic vector potential
$\boldsymbol{A}^f$	Perturbation of magnetic vector potential
$\boldsymbol{A}^u$	Unflawed magnetic vector potential
ϕ	Electric scalar potential
ϕ^f	Perturbation of electric scalar potential
ϕ^u	Unflawed electric scalar potential
$\boldsymbol{B}_0$	Source magnetic induction intensity vector
$\boldsymbol{E}$	Electric field intensive vector
$\boldsymbol{E}^f$	Perturbation of Electric field intensive vector
$\boldsymbol{E}^u$	Unflawed electric field intensive vector
$\widetilde{\boldsymbol{E}}$	Joint electric field intensive vector
μ, μ_0	Permeability of the conductor and free space
$\sigma(\mathbf{r}), \sigma_0$	Conductivity of the conductor and free space

List of Figures

1. Introduction

Shape reconstruction of cracks in a structural component is an important issue for ensuring safety of the whole engineering structure (e.g. steam generator tubing in a power plant of pressurized water reactor). In addition, a reliable prediction of crack profiles is also indispensable in order to extend the ISI (In-Service Inspection) period which, as well known, connects with a huge economic benefit. The conventional ways of non-destructive testing, however, are still difficult to satisfactorily fulfill such a requirement on the quantitative nondestructive evaluation. Hence, great efforts is still necessary for upgrading the present NDT technologies in order that the quantitative inspection can be realized with both a reasonable precision and a high efficiency.

As an effort to enhance the technique of crack reconstruction using eddy current testing (ECT), a database used scheme was recently developed for artificial cracks embedded in a conducting tube by incorporating a novel fast forward solver to a reconstruction algorithm of the conjugate gradient method. The validity of the approach has been verified by reconstructing artificial cracks of electro-discharge machining (EDM) from both simulated and measured ECT signals[1],[2]. To apply this method to the practical inspection of surface breaking natural cracks such as a SCC (Stress Corrosion Crack) or an IGA (Inter-Granular Attack), however, more work is needed for both the modeling of natural cracks and the improvement of inversion algorithm. As described in Ref.[3], the reconstruction of multiple cracks and a crack with non-vanishing conductivity are fundamental steps to realize the inversion of practical natural cracks. Bearing mind these backgrounds, we develop an approach for the reconstruction of a single crack of non-vanishing conductivity in this paper. At first, two numerical models are proposed for describing both the shape and conductivity features of a crack. The rapid simulation of ECT signals arisen from these idealized cracks is considered then by extending the knowledge based fast forward scheme to the case of a touched crack. Thirdly, the crack parameters are solved by using a way of optimization analysis which is developed based on a modified algorithm of the conjugate gradient method and a upgraded code of the rapid forward scheme. Several cracks of typical profiles are successfully reconstructed on a personal computer which in turn, verified the validity of the proposed strategy.

This report is arranged as follows: the numerical modeling of a natural crack is proposed at the next section. The rapid forward scheme and inverse procedure for a cavity crack (EDM notch) are briefly reviewed in the section 3 in order to make the

newly proposed formulae easier to be accepted. The scheme for rapid predication of pick-up signals and related gradients of the idealized natural crack is described at section 4 with an emphasis upon the difference from the formulae for the cavity crack. Section 5 is for description of the inverse analysis. The validation of the methods for both the forward and the inverse analysis is presented at the section of numerical results. The conclusions and discussions are given in the last part.

2. Modeling of a crack with non-vanishing conductivity

As shown in Fig.1, a natural crack usually has a much more complicated geometry than an EDM notch. However, considering features of the fabrication procedure and the application environment, a crack occurred in a SG tube usually appears as an axial or a circumferential one perpendicular to the tube surface. The width of the crack, also, can be assumed varied in a small range. Consequently, it is reasonable to simplify a natural crack as a planar notch of given opening and non-vanishing conductivity at the first step to consider its reconstruction. On the basis of such an assumption, the shape reconstruction of a natural crack becomes a problem to predicate the crack edge curve and/or the conductivity distribution at crack region from the detected pick-up signals.

One of the most direct ways to model a crack is to employ the distribution of conductivity in a selected region which represents the crack edge with a jump of conductivity (hereafter we call it the conductivity model). Usually, such a function of conductivity distribution needs to be discretized in order to treat the crack with a numerical way. A set of box functions is a suitable candidate to be used as the discrete base functions[4],[5]. However, it subjects to a drawback of low approximation order that means a low precision unless enough fine discrete cells are adopted. On the other hand, wavelet functions are recently verified efficient for the expansion of a function with nonstationary property or abrupt change, and the location where jump occurs also can be simply extracted by using the multi-scale analysis technique[6],[7],[8]. Therefore, as the first model for the crack with non-vanishing conductivity, we describe it with a two dimensional function supported within a selected region, and assume the conductivity unchanged in the direction perpendicular to the crack plane. In this case, the distribution of conductivity can be expanded to the following discrete form by employing the Daubechies' wavelet function,

$$\sigma(x,z) = \sum_{k_1}\sum_{k_2} a_{n,k_1k_2}\phi_{n,k_1}(x)\phi_{n,k_2}(z), \tag{1}$$

where, $x \in [-l/2, l/2], z \in [-h/2, h/2]$ with l, h being respectively the length and thickness of the selected region where cracks possibly happen. $\phi_{n,k_1}(x)$ and $\phi_{n,k_2}(z)$ are scaling functions with resolution level n that are expressed by the Daubechies' mother wavelet as $\phi_{n,k}(x) = 2^{n/2}\phi(2^n x - k)$, and k_1, k_2 are shift parameters with ranges,

$$2 - 2N \leq k_1 \leq 2^n - 1 \tag{2}$$

$$2 - 2N \leq k_2 \leq 2^n - 1 \tag{3}$$

and N is the index of the adopted Daubechies' mother wavelet.

Considering the features of a surface breaking SCC crack, treating it by the conductivity distribution model obviously lacks of efficiency as the conductivity model is a general one suitable for any planar flaws. The drawback caused by this wide feasibility is that it may lead to a significant decrement on the condition number of the system equations discretized from the corresponding inverse problem. In fact, by observing the broken tube segments where natural cracks exist, it is easy to find that a crack region of non-vanishing conductivity usually is along the crack edge. If we assume the conductivity in this region does not vary significantly, the model illustrated in Fig.2, i.e., a crack consisting of two regions of different conductivity separated by an extra edge curve, seems a good approximation of the crack we considered (hereafter we call it two-edge model). Although the two-edge model is valid only for a specified case, it is obviously more suitable in applications than the EDM crack (a cavity model of crack), as the later one may gives a much smaller estimation of crack size, if the conductivity in crack region is not zero. The two-edge model can take into account the effect of the touch occurred between the two crack surfaces in the reconstruction procedure by solving both the conductivity and functions describing the two edge curves. In addition, as the two dimensional crack function adopted in the conductivity model is reduced to two 1-d functions, the condition number of the ill-posed inverse problem can be improved significantly. Practically, the crack parameter for this model can be chosen as σ_1, the conductivity at the conducting band region, and $\mathbf{b}$, the coordinate vector of the discrete points of crack edges.

In the following sections, the rapid scheme for forward analysis and the inverse algorithm for parameter optimization will be described respectively for these two crack models. The suitability of these models will be evaluated by applying them to the shape reconstruction with use of simulated ECT signals and signals containing artificial noise.

3. An overview of reconstruction method for an EDM notch

3.1 Basic formulation for a forward problem[1]

Upon subtracting the $A-\phi$ formulae about $\mathbf{A}^u, \phi^u$, the vector and scalar potentials of the unflawed conductor, from those about $\mathbf{A}, \phi$, the potentials of a conductor with flaw present, one can obtain the following governing equations about the field perturbation $\mathbf{A}^f, \phi^f$ for a low frequency eddy current problem,

$$\frac{1}{\mu_0}\nabla^2\mathbf{A}^f - \sigma_0(\dot{\mathbf{A}}^f + \nabla\phi^f) = -[\sigma_0 - \sigma(\mathbf{r})](\dot{\mathbf{A}} + \nabla\phi), \tag{4}$$

$$\nabla\cdot\sigma_0(\dot{\mathbf{A}}^f + \nabla\phi^f) = \nabla\cdot[\sigma_0 - \sigma(\mathbf{r})](\dot{\mathbf{A}} + \nabla\phi), \qquad (in\ conductor) \tag{5}$$

$$\frac{1}{\mu_0}\nabla^2\mathbf{A}^f = 0, \qquad (in\ air) \tag{6}$$

where, $\mathbf{A}^f = \mathbf{A}-\mathbf{A}^u$, $\phi^f = \phi-\phi^u$ are the potential perturbations due to the presence of a crack, σ_0 is the conductivity of the host material and $\sigma(\mathbf{r})$ is the distribution of conductivity that is equal to 0.0 in crack region and σ_0 in the conductor. As $[\sigma_0 - \sigma(\mathbf{r})]$ vanishes in the conducting area, after FEM-BEM discretization, the Eqs.(4)$\sim$ (6) reduces to,

$$\begin{bmatrix} \bar{K}_{11} & \bar{K}_{12} \\ \bar{K}_{21} & \bar{K}_{22} \end{bmatrix} \begin{Bmatrix} q_1^f \\ q_2^f \end{Bmatrix} = \begin{bmatrix} \widetilde{K}_{11} & 0 \\ 0 & 0 \end{bmatrix} \begin{Bmatrix} q_1^f + q_1^u \\ q_2^f + q_2^u \end{Bmatrix}, \tag{7}$$

where, $\{q^f\} = \{\mathbf{A}^f, \phi^f\}^T, \{q^u\} = \{\mathbf{A}^u, \phi^u\}^T$ are the potentials at every node, $[\bar{K}]$ is the coefficient matrix of the unflawed conductor, and $[\widetilde{K}]$ is the coefficient matrix corresponding to the terms with $[\sigma_0 - \sigma(\mathbf{r})]$. The unknown potential vector $\{q\}$ was divided into two parts: $\{q_1\}$ are the potential values at the node of crack element and $\{q_2\}$ are the remained unknowns. As $[\sigma_0 - \sigma(\mathbf{r})]$ vanishes in region $\Omega - \Omega_c$, $[\widetilde{K}]$ is written as in Eq.(7) where the nonzero submatrix $[\widetilde{K}_{11}]$ corresponds to the cells at the crack region.

Multiplying Eq.(7) left by $[H] = [\bar{K}]^{-1}$, we find,

$$\begin{Bmatrix} q_1^f \\ q_2^f \end{Bmatrix} = \begin{bmatrix} H_{11} & H_{12} \\ H_{21} & H_{22} \end{bmatrix} \begin{bmatrix} \widetilde{K}_{11} & 0 \\ 0 & 0 \end{bmatrix} \begin{Bmatrix} q_1^f + q_1^u \\ q_2^f + q_2^u \end{Bmatrix}. \tag{8}$$

The equations related to the unknowns $\{q_1^f\}$ can be simply separated from the

Eq.(8). If we denote $[H_{11}][\widetilde{K}_{11}]$ as $[G]$, and the unit matrix as $[I]$, the relation connecting the unflawed field to the field perturbation in region Ω_c is finally deduced as follows,

$$[I - G]\{q_1^f\} = [G]\{q_1^u\}. \tag{9}$$

As the unknowns of Eq.(9) are limited to the crack region Ω_c, calculation of the disturbed field $\{q_1^f\}$ using this equation is much faster than the conventional FEM-BEM code. This increment of speed comes from the significantly reduced number of unknowns. The information about the conductor and exciting coils are contained in the coefficient matrices $[H_{11}]$ and $\{q_1^u\}$, that can be calculated *a priori* as they are independent of the crack. Thus, once these fields were calculated and stored in data-bases, there is no need to compute them again in the actual calculation of crack fields. Consequently, the computational burden can be reduced significantly.

The basic difference between the Eq.(9) and the conventional schemes using VIM is the different type of unknowns. The application of the potentials makes the interpolation of eddy currents a higher order and makes a new FEM element containing crack edge applicable (this will be explained later). Therefore, the evaluation of a crack which is difficult to be treated by other methods, can be efficiently performed with use of the new scheme.

3.2 Establishment of data-bases

From ECT signal, some features of a crack such as the position, length and inner/outer property usually can be estimated roughly with a classification method. Thus, it is not difficult to choose an area including possible cracks and to subdivide it into a grid of small cells. We calculate the unflawed field at Ω_0 using the conventional FEM-BEM code with the excitation current in the probe or a unit potential acting at one of the nodes in Ω_0 respectively. Storing these results in data-bases, the matrices $[H_{11}]$ and $\{q^u\}$ of Eq.(9), which are necessary for the fast evaluation of ECT signal, can be extracted directly from the data-bases for any cracks contained in the region Ω_0. Here the property was used that the field at the crack region excited by a unit source corresponds to a column of the inverse matrix $[H_{11}]$.

In case of a conducting tube that is sufficiently long relative to the probe dimensions, the size of the data-bases can be greatly reduced by considering the shift property of the electromagnetic field. If the exciting points are in the same layer (same radial coordinate), the fields excited at different axial (or circumferential) lo-

cations will be the same except a shifted axial (or circumferential) coordinate. Thus, we only need to store the field of sources acting at a radial line in the central cross section of the tube. The field due to a unit source at other nodes can be simply found from these data by shifting the coordinates.

3.3 The pick-up signal

As the disturbed field $\{q_i^f\}$ can be considered as the unflawed field induced by current dipoles in crack region, it is convenient to calculate the pick-up signals using the reciprocity theorem[10]. For a self induction pancake coil, the impedance change is written as,

$$\triangle Z = \frac{1}{I^2}\int_{coil} \mathbf{E}^f \cdot \mathbf{J_0} dv = \frac{1}{I^2}\int_{flaw} \mathbf{E}^u \cdot (\mathbf{E}^f + \mathbf{E}^u)(\sigma_0 - \sigma(\mathbf{r}))dv, \qquad (10)$$

where $(\sigma_0 - \sigma(\mathbf{r}))(\mathbf{E}^f + \mathbf{E}^u)$ is the current dipoles in flaw region and I is the current per turn in the coil. The calculation of the impedance with Eq.(10) requires very little computational work as it can be integrated with the help of the known element coefficient matrices directly. The EMF (Electromotive Force) of a mutual induction probe can also be evaluated by using a similar formula. In this case, the fields induced by a virtual current in pick-up coil have to be incorporated[1].

3.4 Introducing of a new FEM element

As the data-base have to be established using the grid of given cells *a priori*, only cracks being made up of the cells can be treated by using these data-bases if homogeneous conductivity is a necessary condition in each FEM element. However, as the permeability and permittivity constants of the SG tubes are the same as those of free space, the electric charge at a conductor surface is negligible small like the neglected displacement current[16] for low frequency problem. Hence, the electromagnetic fields are continuous and the corresponding potentials $\mathbf{A}, \phi$ are approximately one order differentiable at the crack edge. In addition with the fact that small grid cells are usually selected for subdividing Ω_0, it is reasonable to apply the shape function of a normal FEM element in the interpolation of unknown field even for a cell containing crack edge, i.e. with different media. This treatment is similar to what has been proposed in Ref.[17]. Introducing such a new element can enable

us to simply treat cracks with arbitrary shape. In such a case, the difference of the material is taken into account in the element coefficient matrices, as the integration over the whole element is reduced to the part related to the crack region.

3.5 Algorithm for the inverse problem[2]

We define the mean-square residual as,

$$\varepsilon(\mathbf{c}) = \sum_{m=1}^{M} |Z_m(\mathbf{c}) - Z_m^{obs}|^2 \tag{11}$$

where, $\{c\}$ is the vector of crack shape parameters. $z_m(\mathbf{c})$ and z_m^{obs} are the predicted and observed impedance signals at m-th sampling point respectively. The total data number M is equal to the product of the number of scanning points and the number of frequency.

The selection of an object function is very important when noise or model inaccuracies are present. Usually, some weight coefficients or/and some extra constraint conditions are also introduced in the object function in order to avoid the possible local minimum. In the present problem, as we assume that the initial values of the crack position can be chosen as values not too far from the true shape, it is reasonable to regard the the object function as the mean-square error defined by Eq.(11) if S/N ratio is not too small.

We optimize the crack shape vector $\{c\}$ by minimizing the mean-square error with the following iteration,

$$\{c\}_n = \{c\}_{n-1} + a_n\{\delta c\}_n, \tag{12}$$

where $\{\delta c\}_n$ is the update direction of n-th iteration, which is chosen as the direction parallel to the derivative vector $\{\frac{\partial \varepsilon}{\partial c_i}\}$ in the steepest descent algorithm. a_n is a step-size parameter determined as the value maximumly reducing the residual. In the conjugate gradient method, the vector $\{\delta c\}$ in Eq.(12) is adjusted to a new direction by considering the convergence history in order to accelerate the convergence.

To calculate the derivative $\partial\varepsilon/\partial c_i$, it is efficient to apply the method using adjoint field. The formulae of this method are as follows,

$$\frac{\partial \varepsilon}{\partial c_i} = 2Re\left\{\sum_{m=1}^{M}\{Z_m(\mathbf{c}) - Z_m^{obs}\}^* \frac{\partial Z_m(\mathbf{c})}{\partial c_i}\right\}, \tag{13}$$

with the derivatives of impedance signal evaluated with the following equation,

$$\frac{\partial Z_m(\mathbf{c})}{\partial c_i} = -\int_S \mathbf{E}_t^m(\mathbf{r}) \cdot \tilde{\mathbf{E}}_t^m(\mathbf{r}) \frac{\partial s(\mathbf{c},\mathbf{r})}{\partial c_i} \mathbf{n} \cdot \mathbf{k_i} ds, \tag{14}$$

where, $\tilde{\mathbf{E}}$ is the adjoint electric field. $s(\mathbf{c},\mathbf{r})$ is the function and $\mathbf{n}$ the normal unit vector of the crack edge. $\mathbf{k}_i$ is the unit vector parallel to the variation direction of δc_i. The integral region S is a ribbon shaped surface with width equal the crack opening h_0 and along the crack edge. In Eq.(14), the electric field was replaced by its tangential component as no current flows across the conductor surface.

For SG tubing with crack perpendicular to its surface, the field is self-adjoint that can simplify the Eq.(14) further. For step size parameter a_n, it can be calculated with $a_n = P/Q$ and[10],

$$P = Re\left\{\sum_m (Z_m^{n-1} - Z_m^{obs})^* \frac{\partial Z_m^{n-1}}{\partial a_n}\right\}, \qquad Q = \sum_m \left|\frac{\partial Z_m^{n-1}}{\partial a_n}\right|^2. \tag{15}$$

3.6 Shape parameters of an EDM crack

We limit our problem further to the surface breaking cracks considering the property of ECT. Assuming inner/outer and axial/circumferential properties were known from the phase property of ECT signal prior to the inversion, it is reasonable to express the crack with an open piecewise line like the way described in Fig.3. A constraint condition is needed in this discretization to impose the two end points p_1 and p_{n_c} located at the surface of conductor. Written as equation, the discretized edge curve becomes,

$$x(t) = s_1(p_1,...,p_{n_c},t) = x_{p_i} + \frac{x_{p_{i+1}} - x_{p_i}}{t_{i+1} - t_i}(t - t_i), \quad t \in [t_i, t_{i+1}] = \Gamma_i, \tag{16}$$

$$i = 1, 2, ...n_c$$

$$z(t) = s_2(p_1,...,p_{n_c},t) = z_{p_i} + \frac{z_{p_{i+1}} - z_{p_i}}{t_{i+1} - t_i}(t - t_i), \quad t \in [t_i, t_{i+1}] = \Gamma_i, \tag{17}$$

$$i = 1, 2, ...n_c - 1$$

where $p_1, .., p_{n_c}$ are n_c points equally spaced at the crack edge. x_{p_i}, z_{p_i} and t_i are the rectangular and curve coordinates of the point p_i respectively. The first and last points are located at the corresponding surface point with same x value. The

variation of the edge is expressed by the variation of coordinates as follows,

$$\delta s(\mathbf{c},\mathbf{r}) = \delta \mathbf{r} = \delta s_1(\mathbf{c},t)\mathbf{i} + \delta s_2(\mathbf{c},t)\mathbf{k} = \sum_i \frac{\partial s_1(\mathbf{c},t)}{\partial x_{p_i}} \delta x_{p_i}\mathbf{i} + \sum_i \frac{\partial s_2(\mathbf{c},t)}{\partial z_{p_i}} \delta z_{p_i}\mathbf{k}, \quad (18)$$

where, $\mathbf{i},\mathbf{k}$ denote the unit vectors along the x and z direction. Substituting Eq.(18) into Eq.(14) with $\partial s_1(\mathbf{c},t)/\partial x_{p_i}$ and $\partial s_2(\mathbf{c},t)/\partial z_{p_i}$ derived from Eqs.(16) and (17), the derivatives of the impedance Z_m are expressed in term of the electric field by the following integrals,

$$\frac{\partial Z_m}{\partial x_{p_i}} = -\sigma_0 \int_{-\frac{h_0}{2}}^{\frac{h_0}{2}} \left\{ \int_{\Gamma_i} E_{mt}^2 \frac{(t_{i+1}-t)}{(t_{i+1}-t_i)} \frac{(z_{p_{i+1}}-z_{p_i})}{(t_{i+1}-t_i)} dt + \int_{\Gamma_{i-1}} E_{mt}^2 \frac{(t-t_{i-1})}{(t_i-t_{i-1})} \frac{(z_{p_i}-z_{p_{i-1}})}{(t_i-t_{i-1})} dt \right\} dy,$$

$$i = 1, 2, \ldots\ldots n_c \quad (19)$$

$$\frac{\partial Z_m}{\partial z_{p_i}} = -\sigma_0 \int_{-\frac{h_0}{2}}^{\frac{h_0}{2}} \left\{ \int_{\Gamma_i} E_{mt}^2 \frac{(t_{i+1}-t)}{(t_{i+1}-t_i)} \frac{(x_{p_i}-x_{p_{i+1}})}{(t_{i+1}-t_i)} dt + \int_{\Gamma_{i-1}} E_{mt}^2 \frac{(t-t_{i-1})}{(t_i-t_{i-1})} \frac{(x_{p_{i-1}}-x_{p_i})}{(t_i-t_{i-1})} dt \right\} dy,$$

$$i = 2, 3, \ldots\ldots, n_c - 1 \quad (20)$$

where, the integration along the thickness direction of crack is carried out with the variable y from $-h_0/2$ to $h_0/2$.

If the crack parameter c_i was chosen as the step length of the modification along the normal direction of the crack edge as shown in Fig.3, the derivative with respect to this parameter can be obtained by imposing the point p_i move along the normal direction. Thus, the derivative with respect to c_i is equal to the partial derivative at the normal direction $\mathbf{n}_{p_i}$,

$$\frac{\partial Z_m}{\partial c_i} = \nabla Z_m \cdot \mathbf{n}_{pi} = \frac{\partial Z_m}{\partial x_{p_i}} n_{x_{p_i}} + \frac{\partial Z_m}{\partial z_{p_i}} n_{z_{p_i}}. \quad (21)$$

Moreover, we only need to choose the point number $n_c = 4$ for dealing with a rectangular crack. In this case, the derivatives with respect to the independent crack parameters (such as, the depth of the crack and the x coordinate of the two ends) can be obtained from the derivatives of Eqs.(19) and (20) using the transform matrix $[T]$ as,

$$\left\{ \frac{\partial Z_m}{\partial c_i} \right\} = [T] \left[\left\{ \frac{\partial Z_m}{\partial x_{p_i}} \right\}^T, \left\{ \frac{\partial Z_m}{\partial z_{p_i}} \right\}^T \right]^T. \quad (22)$$

4. Extension of the fast forward strategy

Theoretically, the forward scheme developed for predicting ECT signals of a cavity crack is also suitable for a crack with non-vanishing conductivity if the element with multiple media[1] is applicable for treating the change of conductivity. However, in case of models for a natural crack, much more complicated distribution of conductivity may happen in an element. Even for the two-edge model, different combinations of the edge curves also may lead to a complex distribution in an element containing part of the crack edges. Therefore, modifications are necessary in order that the analysis code for a cavity crack can be extended to the problem of distributed conductivity. In this section, we derive basic formulae for the fast simulation of the signals coming from the two models separately with the emphasis placed on the difference with the procedure for a cavity crack.

4.1 Formulation for the conductivity model

If we assume the conductivity changing smoothly at the crack region besides the crack edge, the formulae for a cavity crack can be extended without much modifications. As the difference between a cavity crack and a crack with non-vanishing conductivity occurs only in the distribution of conductivity, we can treat a crack of the conductivity model by taking this difference into account in the coefficient matrix $[K]$ of Eq.(9), the only term possibly affected by the distribution of $\sigma_0 - \sigma(\mathbf{r})$. Practically, the conductivity in the formulae for each sub-matrix of $[K]$ should be considered as a variable[2]. Taking sub-matrix $[N_2]$ as an example, it becomes,

$$[N_2] = \int_{\Omega_c} (\sigma_0 - \sigma(\mathbf{r}))[N][N]^T dv, \tag{23}$$

where $[N]$ is the matrix of shape function of FEM by which the potentials are discretized. The integral in Eq.(23) can be simply calculated with use of the Gauss integration by treating the conductivity as a variable at each Gauss point like,

$$[N_2] = \sum_l \sum_m \sum_n w_l w_m w_n (\sigma_0 - \sigma(\mathbf{r}_{lmn}))[N(\mathbf{r}_{lmn})][N(\mathbf{r}_{lmn})]^T, \tag{24}$$

where, w_l, w_m, w_n are the weight coefficients, and $\mathbf{r}_{lmn}$ is the coordinate vector corresponding to the $lnm - th$ Gauss point.

The derivatives with respect to the coefficients of the wavelet expansion can be

derived with use of the equation given in Ref.[9],[10] by replacing the base function as the scaling function of Daubechies' wavelet. Considering the compact support property of the wavelet function, the integral becomes,

$$\frac{\partial Z_m}{\partial a_{n,k_1k_2}} = \int_{-h}^{h}\{\int_{S_{k_1k_2}} (\sigma_0 - \sigma(r))|\mathbf{E}_m(x,y,z)|^2\phi_{k_1}(x)\phi_{k_2}(z)dxdz\}dy, \qquad (25)$$

where, $S_{k_1k_2}$ is the joint area of the support of the two dimensional wavelet $\Phi_{n,k_1k_2}(x,z)$ $= \phi_{n,k_1}(x)\phi_{n,k_2}(z)$ and the selected zone of crack. The ranges of the subscripts k_1 and k_2 are the same as those given in Eq.(2) and (3). The Eq.(25) can also be calculated by applying the Gauss integration to each subregion selected according to the resolution level of the wavelet bases.

4.2 Formulation for the two-edge model

The two-edge model is a specific case of the conductivity model. Therefore, the calculation of the pick-up signals can be performed with a similar way like those just stated. However, as the description of the crack has been modified, a new formulation is necessary for predicting the gradients. In addition, it is more efficient if we take the features of the two-edge model into account during the forward analysis as it possibly be separated into two problems of a cavity crack. This property can simplify the implement procedure of the derived formulae as the code for a cavity crack is applicable directly. Follows is the basic formulation corresponding to this idealized model of a natural crack.

For the forward analysis of a crack of the two-edge model, it is easy to find that the coefficient matrix $[H]$ in Eq.(9) has no difference with that for a cavity crack or a crack of the conductivity model if the analysis region was selected the same. At the same time, in spite of the effects of crack shapes on the coefficient matrix $[K]$, this matrix can be derived from the coefficient matrices of two cavity cracks defined respectively by the two edge curves. Similarly, the gradients with respect to the crack parameters of the two-edge model can also be derived from the gradients corresponding to the two cavity cracks respectively.

Keeping in mind the property of linear dependence of the coefficient matrix $[K]$ on the conductivity, we can find that each element coefficient matrix contained in

$[K]$ can be expressed as the following equation,

$$[K]_e = \frac{\sigma_1}{\sigma_0}[K_1]_e + \frac{(\sigma_0 - \sigma_1)}{\sigma_0}[K_2]_e = \alpha_1[K_1]_e + (1-\alpha_1)[K_2]_e, \tag{26}$$

where, $[K_1]_e$ is the element coefficient matrix for the cavity crack surrounded by the inner edge, $[K_2]_e$ is of that defined by the outer edge, and $\alpha_1 \equiv \sigma_1/\sigma_0$.

To calculate the gradient with respect to crack parameters of the two-edge model, we can apply the formulae for a cavity crack [Eq.(19),(20] to each discrete point at the two edge curves, with the electric-field adopted as those calculated using the coefficient matrix given in Eq.(24). Denoting the gradient for the crack surrounded by the inner edge as $\partial\bar{Z}_1/\partial b_{1,i}$ and those defined by the outer edge as $\partial\bar{Z}_2/\partial b_{2,i}$, they can be obtained from the following equations in addition with a linear coordinate transformation[2],

$$\begin{aligned}\frac{\partial\bar{Z}_m}{\partial x_{p_i}} &= -\sigma_0 \int_{-h/2}^{h/2}\int_{\Gamma_i} |\mathbf{E}_{tm}|^2 \frac{(t_{i+1}-t)}{(t_{i+1}-t_i)}\frac{(z_{p_{i+1}}-z_{p_i})}{(t_{i+1}-t_i)}dtdy \\ &+ \int_{-h/2}^{h/2}\int_{\Gamma_{i-1}} |\mathbf{E}_{tm}|^2 \frac{(t-t_{i-1})}{(t_i-t_{i-1})}\frac{(z_{p_i}-z_{p_{i-1}})}{(t_i-t_{i-1})}dtdy, \\ & i = 1, 2, ...n_c \end{aligned} \tag{27}$$

$$\begin{aligned}\frac{\partial\bar{Z}_m}{\partial z_{p_i}} &= -\sigma_0 \int_{-h/2}^{h/2}\int_{\Gamma_i} |\mathbf{E}_{tm}|^2 \frac{(t_{i+1}-t)}{(t_{i+1}-t_i)}\frac{(x_{p_i}-x_{p_{i+1}})}{(t_{i+1}-t_i)}dtdy \\ &+ \int_{-h/2}^{h/2}\int_{\Gamma_{i-1}} |\mathbf{E}_{tm}|^2 \frac{(t-t_{i-1})}{(t_i-t_{i-1})}\frac{(x_{p_{i-1}}-x_{p_i})}{(t_i-t_{i-1})}dtdy, \\ & i = 2, 3, ..., n_c - 1 \end{aligned} \tag{28}$$

the actual gradients for a crack of the two-edge model can be predicted by using the following equations, i.e., for points located at the edge of outer side,

$$\frac{\partial Z_m}{\partial b_{1,i}} = \frac{\sigma_1}{\sigma_0}\frac{\partial\bar{Z}_{1,m}}{\partial b_{1,i}} = \alpha_1\frac{\partial\bar{Z}_{1,m}}{\partial b_{1,i}}, \tag{29}$$

for those at the inner edge,

$$\frac{\partial Z_m}{\partial b_{2,i}} = \frac{\sigma_0 - \sigma_1}{\sigma_0}\frac{\partial\bar{Z}_{2,m}}{\partial b_{2,i}} = (1-\alpha_1)\frac{\partial\bar{Z}_{2,m}}{\partial b_{2,i}}. \tag{30}$$

In these equations and those at follows, the subscript m denotes the number representing the order of sampling points of ECT data which is equal to the product of scanning steps and the number of applied frequency.

For α_1, the parameter of conductivity, one has,

$$\frac{\partial Z_m}{\partial \alpha_1} = \sigma_0 \int_{-h/2}^{h/2} \left\{ \int_{S_2} |\mathbf{E}_m|^2 \Phi_{n,k_1k_2}(x,z) dxdz \right\} dy$$

$$- \sigma_0 \int_{-h/2}^{h/2} \left\{ \int_{S_1} |\mathbf{E}_m|^2 \Phi_{n,k_1k_2}(x,z) dxdz \right\} dy \tag{31}$$

or,

$$\frac{\partial Z_m}{\partial \alpha_1} = \frac{\partial \bar{Z}_{m,2}}{\partial \alpha_1} - \frac{\partial \bar{Z}_{m,1}}{\partial \alpha_1}. \tag{32}$$

In case of a crack like that illustrated in Fig.3, the expressions of the gradients with respect to the parameters described in the figure are as follows,

$$\frac{\partial Z_m}{\partial b_i} = \frac{\sigma_1}{\sigma_0} \frac{\partial \bar{Z}_{m,2}}{\partial b_{1,i}} = \alpha_1 \frac{\partial \bar{Z}_{m,2}}{\partial b_{1,i}}, \tag{33}$$

$$\frac{\partial Z_m}{\partial b_{i+3}} = \frac{\sigma_1}{\sigma_0} \frac{\partial \bar{Z}_{m,2}}{\partial b_{1,i}} + \frac{\sigma_0 - \sigma_1}{\sigma_0} \frac{\partial \bar{Z}_{m,1}}{\partial b_{2,i}} = \alpha_1 \frac{\partial \bar{Z}_{m,2}}{\partial b_{1,i}} + (1-\alpha_1) \frac{\partial \bar{Z}_{m,1}}{\partial b_{2,i}}, \tag{34}$$

$$\frac{\partial Z_m}{\partial \alpha_1} = \frac{\partial \bar{Z}_{m,2}}{\partial \alpha_1} - \frac{\partial \bar{Z}_{m,1}}{\partial \alpha_1}, \tag{35}$$

$$i = 1, 2, 3.$$

On the basis of Eqs.(33), (34), (35), we developed a code for the rapid calculation of signals and their corresponding gradients for the idealized cracks. The validity of this approach has been verified by comparing its numerical results with those of the conventional FEM-BEM hybrid code which has been verified accurate for ECT problems through a long term of validations and applications[11],[12]. Fig.4 depicts a comparison of the impedance signals calculated by using the FEM-BEM hybrid code and those of the present rapid scheme. Good agreement is obtained within a much shorter CPU time which, in turn, verified the validity and efficiency of our new scheme. The small difference comes from the adopted different numbers of mesh layers which is difficult to be a large number for the FEM-BEM code because of the limited computer resources.

5. Inverse procedure

According to features of the pick-up signals, it is not difficult to determine an area where a natural crack possibly exist in the conductor to be inspected. This region then can be applied for the establishment of the data-bases needed by the fast forward solver. On the basis of these pre-calculated data, the pick-up signals and the corresponding gradients can be predicted utilizing the formulae proposed in the last section for a given crack. Therefore, in order to solve the crack parameters from an inverse problem, we only need to introduce an algorithm keeping in mind the fact that the pick-up signals and gradients have been known prior to each iteration step.

As both of the pick-up signals and gradients can be efficiently predicted by using the fast forward solver, here we choose the conjugate gradient method for the reconstruction of crack parameters as what has been done in the case for a cavity crack[13],[14],[15]. The crack parameters, on the other hand, are chosen as the coefficients of wevelet expansion for the conductivity model and the coordinates of discrete points at crack edge in addition with the unknown conductivity for the two-edge model.

5.1 A crack of the conductivity model

The objective of the optimization of crack parameters is to minimize the difference between the observed and predicted pick-up signals. Usually, the square residual of the observed and the simulated signals subjected to some constraint conditions is adopted as the object function. For a crack of the conductivity model, the conductivity at the boundary of the selected crack region is equal to the value of the base material. This condition can be selected as constraints upon the square residual, i.e. we impose the coefficients of the discrete expansion to satisfy the boundary condition at points located at the crack edge,

$$f_i = \sum_{k_1=-2N+2}^{-1} \sum_{k_2=-2N+2}^{2^n-1} a_{n,k_1k_2}\phi_{n,k_1}(-1)\phi_{n,k_2}(z_i) = 0, \tag{36}$$

$$g_i = \sum_{k_1=-2N+2}^{-1} \sum_{k_2=-2N+2}^{2^n-1} a_{n,k_1k_2}\phi_{n,k_1}(1)\phi_{n,k_2}(z_i) = 0, \tag{37}$$

$$h_i = \sum_{k_1=-2N+2}^{2^n-1} \sum_{k_2=-2N+2}^{-1} a_{n,k_1k_2}\phi_{n,k_1}(x_i)\phi_{n,k_2}(1) = 0, \tag{38}$$

$$i = 1, 2, ...2^n + 2N - 2,$$

where, the selected zone of a crack has been transformed into a square region with side length equal 2 and with its center located at the coordinate original point. The points used in the above equations, say, $(-1, z_i), (1, z_i), (x_i, 1)$, are equally spaced at the edges of the square besides that in the side of crack opening.

These equations are very strong constraint conditions for the procedure determining the coefficients of conductivity distribution. This may worsen the condition number of inverse problem and lead to failure in convergence. A way to avoid this difficulty is to apply the method of moment, i.e. instead of Eqs.(36), (37), (38), we impose them to be satisfied from the point of view of a weighted average. By multiplying wavelet bases $\phi_{n,k_1}(x)$ (or $\phi_{n,k_2}(z)$) to the two sides of Eqs.(36), (37), (38) and taking integration, the following conditions can be obtained as a weaken form of the constraint conditions,

$$f_{k_2} = \sum_{k_1=-2N+2}^{-1} a_{n,k_1k_2}\phi_{n,k_2}(0) = 0, \tag{39}$$

$$g_{k_2} = \sum_{k_1=-2N+2}^{-1} a_{n,k_1k_2}\phi_{n,k_2}(1) = 0, \tag{40}$$

$$h_{k_1} = \sum_{k_2=-2N+2}^{-1} a_{n,k_1k_2}\phi_{n,k_2}(0) = 0, \tag{41}$$

$$k_1, k_2 = 2 - 2N, ...2^n - 1,$$

where, the orthogonal property of wavelet bases has been applied.

The Eqs.(39), (40), (41) can be taking into account in the object function by using the Lagrange multiplier method as,

$$\varepsilon = \sum_m w_m \left|[Z_m(\mathbf{b}) - Z_m^{obs}]\right|^2 + \sum_i |(\alpha_i f_i + \beta_i g_i + \lambda_i h_i)| \tag{42}$$

where, $Z_m(\mathbf{b})$ is the impedance signals at m-th sampling point arisen from a crack with a parameter vector $\mathbf{b}$ predicted at the previous step. Z_m^{obs} is the observed impedance signals from ECT inspection. Coefficients $\alpha_i, \beta_i, \lambda_i$ are the Lagrange multipliers that can be treated with a similar way like that for the crack parameters.

Actually, the reconstructed conductivity at edges of the selected region has no significant difference if the selected region is enough large comparing with the true crack. In this case, the constraint conditions do not affect the optimization procedure notably. Therefore, it is reasonable to neglect the effect of these extra terms in the

object function if we choose a larger analysis region.

The coefficient of conductivity can be determined with an iteration algorithm of the conjugate gradient method by minimizing the object function (42) or that with the constraint conditions neglected. However, as we have to reconstruct all the coefficient at each iteration step, the analysis area at every step must be taken as the whole selected region. This obviously will result in a large computation burden even for a conductivity change localized in a small area.

5.2 Reconstruction of a crack of the two-edge model

For the reconstruction of a crack of the two-edge model, the algorithm of the conjugate gradient method is also valid after some modifications. In this case, we take the object function as the residual square again and updating the crack parameters partly along the direction of gradient vector. In the follows, we give this inverse algorithm with an emphasis upon the difference with the scheme for a cavity crack[2].

As the first step of the inversion, we need to select an appropriate initial profile for the crack. This is not difficult as we can simply find a cavity crack who gives an impedance signal similar to the measured data by using the code developed for an EDM crack. This procedure is very fast as only discrete points at one edge curve need to be determined. Using the parameters of the selected cavity crack, the initial values of the two-edge model can be chosen by, (1) set the outer edge as the same as the edge of the cavity crack just decided, (2) set the inner crack as that determined by the outer edge and a given band width, and (3) set the initial value of the conductivity parameter as a value around 0.5.

Comparing with the case of a cavity crack, the most significant difference in the iteration procedure is that two types of crack parameter are necessary to be reconstructed, viz, the size of the crack and the conductivity. It is easy to find that, as the units of these two types of parameter are different, the gradient with respect to these parameters may be very different (even much different order). This will lead to a quite different convergent speed for these two types of parameter if a normal algorithm of conjugate gradient method is applied directly. To overcome this difficulty, here we propose a scheme by improving the optimization algorithm. The basic ideas of this procedure is that, the updating direction and step size will be calculated separately for the parameters in different type by partly using the formulae of the conjugate gradient method.

For the parameters related to the crack size, i.e. the coordinate of the two-crack edges, corresponding to the modification direction of gradient $\{\partial\varepsilon/\partial b_i\}$, the formula for the step length a_1^n is,

$$a_1^n = P_1^n / Q_1^n \tag{43}$$

where,

$$P_1^n = Re\left\{\sum_m [Z_m^{n-1}(\mathbf{b}, \alpha_1) - Z_m^{obs}]^* \sum_i \frac{\partial Z_m^{n-1}}{\partial b_i} \frac{\partial \varepsilon^{n-1}}{\partial b_i}\right\} \tag{44}$$

$$Q_1^n = \sum_m \left| \sum_i \frac{\partial Z_m^{n-1}}{\partial b_i} \frac{\partial \varepsilon^{n-1}}{\partial b_i} \right|^2 \tag{45}$$

For step length related to the parameter of conductivity at the band region surrounding the crack, it becomes,

$$a_2^n = P_2^n / Q_2^n \tag{46}$$

where,

$$P_2^n = Re\left\{\sum_m [Z_m^{n-1}(\mathbf{b}, \alpha_1) - Z_m^{obs}]^* \frac{\partial Z_m^{n-1}}{\partial \alpha_1} \frac{\partial \varepsilon^{n-1}}{\partial \alpha_1}\right\} \tag{47}$$

$$Q_2^n = \sum_m \left| \frac{\partial Z_m^{n-1}}{\partial \alpha_1} \frac{\partial \varepsilon^{n-1}}{\partial \alpha_1} \right|^2 \tag{48}$$

Based on the formulae above, the iteration equation for updating the crack parameters can be written as,

$$\{\mathbf{b}^n, \alpha_1^n\}^T = \left\{\mathbf{b}^{n-1} + a_1^n \{\frac{\partial Z_m^{n-1}}{\partial b^{n-1}}\}, \alpha_1^{n-1} + a_2^n \frac{\partial Z_m^{n-1}}{\partial \alpha_1^{n-1}}\right\}^T . \tag{49}$$

6. Implementation and numerical results

On the basis of the formulae described in the previous sections, two codes have been developed respectively for the conductivity model and the two-edge model. In this part we present some typical reconstruction results of these two codes for validating the proposed method. The feasibility and efficiency of the method related to the two models are compared finally from the point of view of possible applications to the inspection of SG tubing.

We choose a self induction pancake coil of 100 turns as the probe for ECT inspection which was winded with an outer radius 1.6 mm, an inner radius 0.5 mm and a thickness 1 mm. The probe is arranged in parallel over the inner surface of tube with a lift-off equal to 1. mm. The excitation frequency is chosen as 400kHz which is a typical one in the practical inspection of SG tubing. The scanning is performed axially along the crack from -10 mm to 10 mm and with the step length chosen as 0.5 mm. These 41 impedance data are used for the reconstruction of all the crack parameters. As a need of the fast forward solver, two data-bases are established with the possible crack region selected as a $10mm \times 1.27mm \times 0.2mm$ cubic zone and subdivided into $20 \times 8 \times 1$ cells.

6.1 Results for the two-edge model

To investigate the efficiency of the two-edge model, we have implemented the algorithm at first for the crack parameters described in Fig.4. For a crack with arbitrary shape, this code can be simply extended by changing the number of crack parameters. In order to validate the algorithm for different type of parameters, the size parameters of the crack are reconstructed in both the conditions of a known and an unknown conductivity parameter. The results show that, the modified scheme of the conjugate gradient method can give satisfactory reconstruction even for the case with different types of parameter.

Fig.6 depicts a comparison of the impedance signals arisen from a reconstructed crack and the simulated impedance which we used as the observed data. The true shape of the crack, as shown in Fig.7, is assumed to be an inner one with a maximum depth equal to 50% of the tube thickness. In this case, the conductivity parameter α_1 at the conducting band region was taken as a known value (=0.5). Excellent reconstruction results are obtained in this case though the convergence speed is not as fast as the case of a cavity crack. The results shown in Fig.6 and Fig.7 are

obtained at the 300-th iteration. The CPU time used is about 3 hours on a personal computer(Gateway GP6-333).

Fig.8 and Fig.9 shows another reconstruction results for a crack with an unknown conductivity after 300 iterations. The reconstructed conductivity parameter is 0.102 for a true value of 0.1. In this case, we chose the initial conductivity as half of the base conductor and start the iteration from the initial crack size predicted by using the code for a cavity crack. The modified algorithm was adopted to update the two types of parameter respectively. Very good convergence result is found again for both the shape parameters and the conductivity. From the satisfactory reconstruction results given here, we come to a conclusion that the reconstruction of crack parameters of different types is possible.

Comparing with the reconstruction of a cavity crack, the iteration number of the present method is much larger for a similar accuracy (over 10 times). This decrement of convergence speed is considered caused by the greatly increased number of local minimum. In other word, the signals from different set of parameters may be very similar although the parameter is much different. This leads to that the step size of updating becomes a small value. From this point of view, more effort is necessary in the near future to accelerate the convergence in order this method possibly to be applied more efficiently in the practical data processing.

6.2 Results for the conductivity model

In Fig.10 and Fig.11, the reconstructed results using the conductivity model are depicted. The iteration number and CPU time corresponding to these results are respectively 100 and over 16 hours on the same personal computer. The significantly increased computational work is caused by the large number of unknowns, as field at the whole selected crack region must be solved at each iteration. In addition, the large number of crack parameters also enlarges the computation burden for estimating the gradient vector. In these results, the resolution level was used as 4 and the index of the Daubechies' wavelet was chosen as 5. The true profiles of the crack is the same as that described in the Fig.9. One can find the shape of the crack approximately from the estimated distribution of conductivity given in Fig.10. However, the jump of conductivity at the crack edge has not been recovered well. This means that it is not very efficient of the conductivity model to reconstruct a crack with an abrupt conductivity jump without much more iterations. This is

because that, even for an impedance signal very similar to that arisen from the true crack, the corresponding conductivity may show much bigger error comparing with the true distribution.

Comparing with the results of the two-edge model, reconstructing conductivity directly is obviously not efficient and accurate especially for a crack with a conductivity jump. Therefore, for the reconstruction of a SCC in SG tubing, using the two-edge model is reasonable.

6.3 Effect of random noise

To consider the robustness of the present inverse scheme, the reconstruction is undertaken with observed data added by artificial noise in this part. By adjusting the maximum value of the noise component, we find that the new inverse scheme can give acceptable estimation of crack shapes even for signals with 20% noise.

In calculation, the observed ECT data Z^{sobs} was generated with the following formula which combines the simulated ECT data Z^{sim} with a white noise,

$$Z_m^{sobs} = Z_m^{sim} + \alpha |Z_{max}^{sim}| \xi_m, \tag{50}$$

where, α is the proportion of the noise in the whole signal, ξ_m is random values within $[-1.0, 1.0]$ and is generated by a short computer code of the white noise, $|Z_{max}^{sim}|$ is the maximum value of the simulated ECT data.

In Fig.12 and Fig.13, the reconstructed crack shape and impedance signals are compared with the true ones. In this case, the true crack is selected the same as that utilized in Fig.8 and Fig.9 again. 5% white noise was added to the observed signals. It is easy to find that, although the reconstruction precision is not as high as the case without noise included, satisfactory crack parameters are obtained with a similar computational burden. The reconstructed value of the conductivity is 0.144 with the true value used as 0.1, the same as the case of Fig.8 and Fig.9. Fig.14 and Fig.15 depict the reconstructed crack shape and impedance signals in case of 10% noise. Satisfactory crack parameters are predicted again within a similar computational time.

7. Conclusions

In this paper, by proposing new models for a stress corrosion crack and extending the inverse scheme of a cavity slit, the reconstruction of an idealized natural crack with non-vanishing conductivity was successfully realized at a personal computer. The simulation results depicted that the model with two edges and unknown constant conductivity is better than the conductivity model in efficiency and more suitable for the practical problems. By performing reconstruction with use of signals containing artificial noise, the new approach was demonstrated both robust and feasible for predicting profiles of the idealized crack model. More work is necessary for investigating the efficiency of the present method for a measured signal and for the problem with an unknown position of crack plane.

8. References

[1] Z.Chen, K.Miya, and M.Kurokawa, Rapid prediction of eddy current testing signals using $\mathbf{A} - \phi$ method and database, NDT&E international, Vol.32, No.1, 29-36, 1998.

[2] Z.Chen and K.Miya, ECT inversion using a knowledge based forward solver, J. Nondestr. Eval., Vol.17, No.3, 157-165, 1998.

[3] Z.Chen, W.Cheng and K.Miya, Shape reconstruction of natural cracks using a fast forward solver, in Proc. of 2-nd Japanese-French Joint Seminar on Eddy Current NDT, 104-111, 1997.

[4] Z.Badics et al., Rapid flaw reconstruction scheme for 3-d inverse problems in eddy current NDE, in Stud. Appl. Electromagn. Mech., Vol.12, 303-309, eds. T.Takagi et al., IOS press, 1996.

[5] H.A.Sabbagh and L.D.Sabbagh, Inverse problems in electro-magnetic non-destructive evaluation, Int. J. of Appl. Electromagn. in Mater. V.3, 253-261, 1993.

[6] Daubechies, Orthonormal bases of compactly supported wavelet, Commun. Pure Appl. Math., 41, 909-996, 1988.

[7] G.Mallat, A theory for Multiresolution Signal decomposition: the wavelet representation, Commun. Pure Appl. Math., 41, 674-693, 1988.

[8] Z.Chen, Y.Yoshida and K.Miya, Analysis of relations between the defect shapes and the wavelet coefficients of ECT data, in Studi. Appl. Electromagn. Mech., Vol.8, eds. R.Collins and et al., IOS press, 295-302, 1995.

[9] S.Norton and J.Bowler, Theory of ECT inversion, J. Appl. Phys. Vol.73, No.2, 501-512, 1993.

[10] J.R.Bowler, Eddy current interaction with an idea crack, I. the forward problem, J. Appl. Phys. Vol.75, No.12, 8128-8137, 1994.

[11] M.Kurokawa, K.Suguyama and K.Miya, An inverse analysis with the current vector potential $\mathbf{T}$, in Simulation and Design of Applied Electromagnetic Systems, Ed., T.Honma, Elsevier, 197-200, 1994.

[12] T.Takagi, et al, Benchmark models of eddy current testing for steam generator tube: experiment and numerical analysis, Int. J. Appl. Electromagn. in Materials, Vol.4, 149-162, 1994.

[13] L.Udpa and S.S.Udpa, eddy current defect characterization using neural networks, Mater. Eval. Vol.48, No.1, 50-54, 1990.

[14] R.Zorgati and et al, eddy current testing of analyses in conductive materials, II. Quantitative imagine via deterministic and stochastic inversion technique, IEEE Tran. Magn., Vol.28, No.3, 1850-1862, 1992.

[15] J.Pavo and K. Miya, Reconstruction of crack shape by optimization using eddy current field measurement, IEEE Trans. on Mag., Vol.30, No.5, 3470-3410, 1994.

[16] J.A.Tegopoulos and E.E.Kriezis, Eddy currents in linear conducting media. Elsevier Science Publisher, 1985.

[17] M.Gramz, and et al., A crack element concept for a FEM analysis of eddy current distribution in a long cylinderical bar with a crack, in Nondestructive Testing (Proceedings of the 12^{th} world conference), Opsit, p1035, 1989.

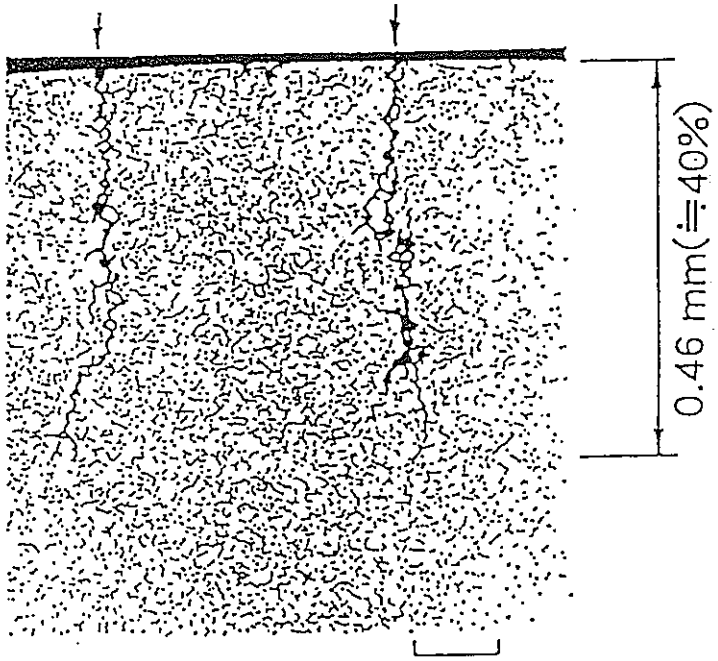

Fig.1 A viewgraph of typical SCC cracks in a SG tube

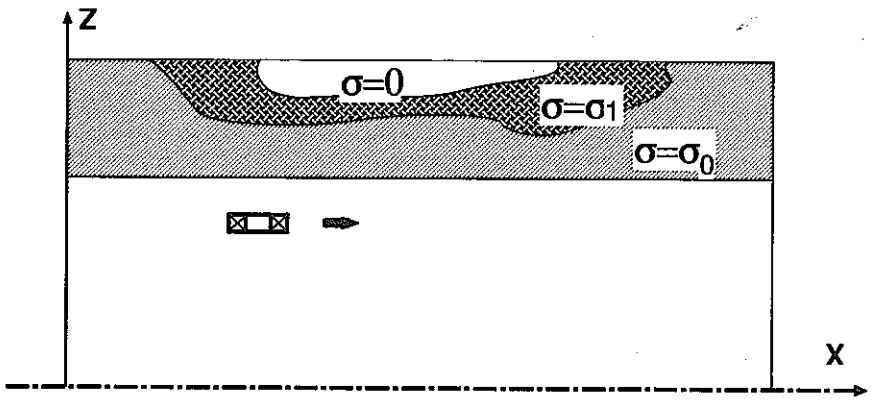

Fig.2 The two-edge model for a crack with touch

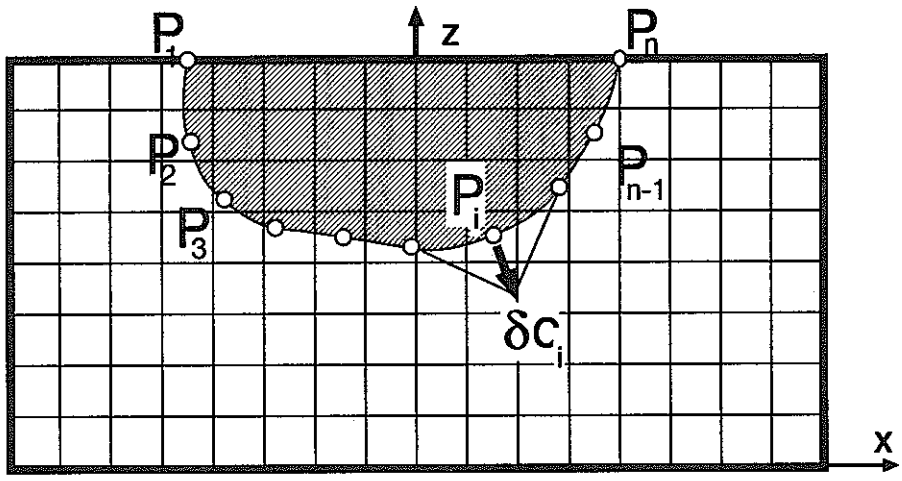

Fig.3 Discret parameters of an EDM crack

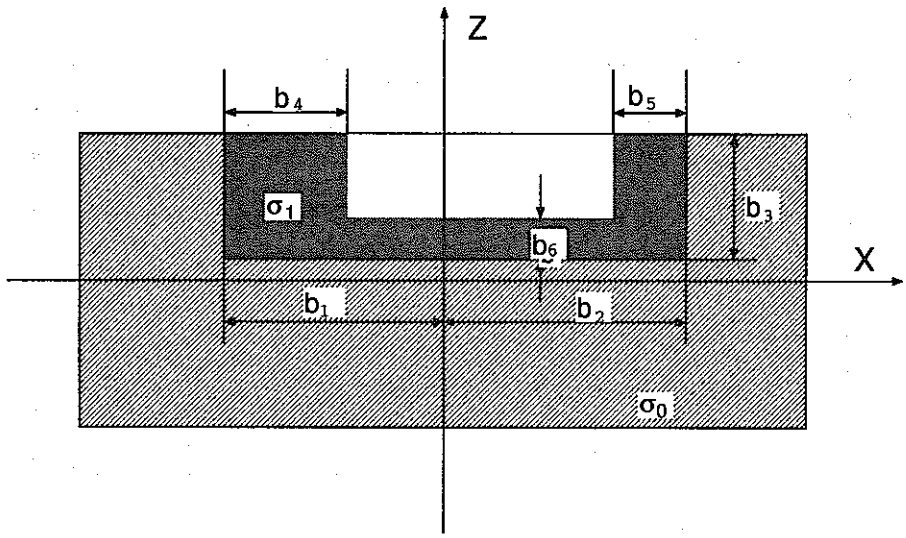

Fig.4 Crack parameters of two-edge model in case of a rectangular crack

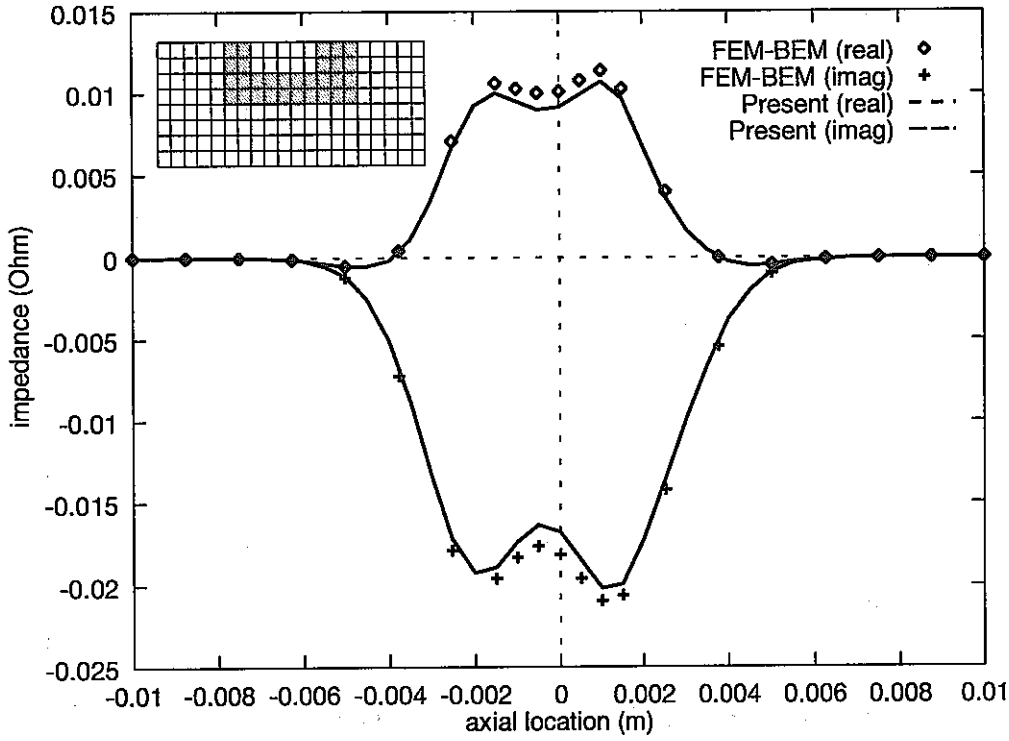

Fig.5 Comparison of simulated impedance signals by the FEM-BEM code and by the present method

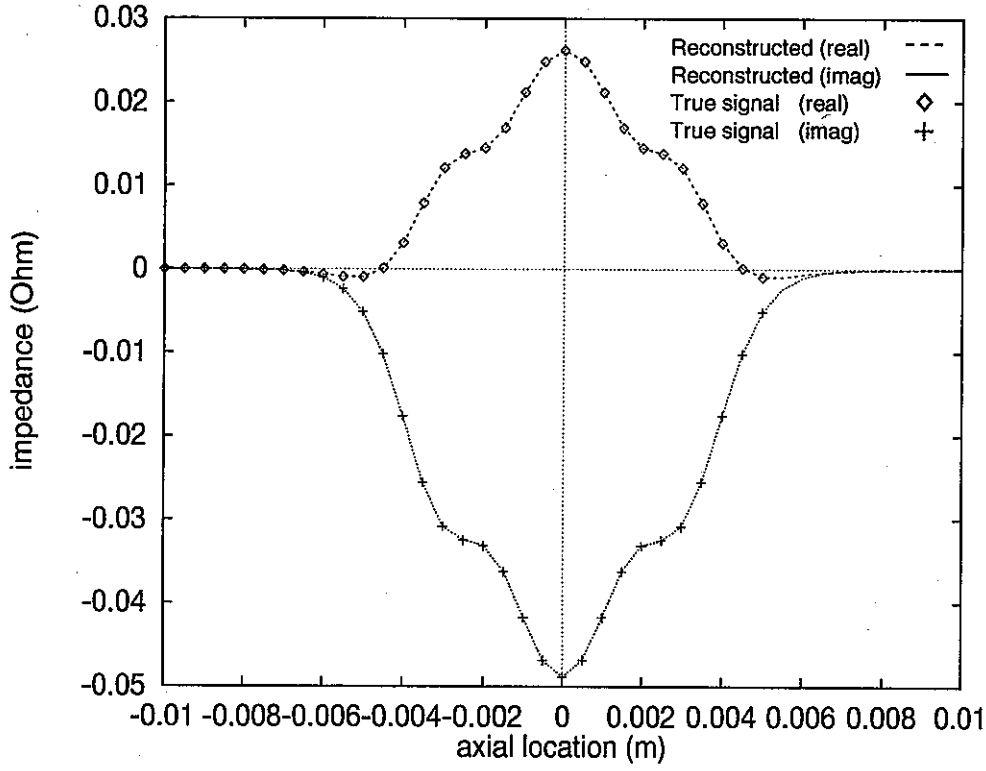

Fig.6 Impedance signals due to the reconstructed crack
(known conductivity of the conducting band region)

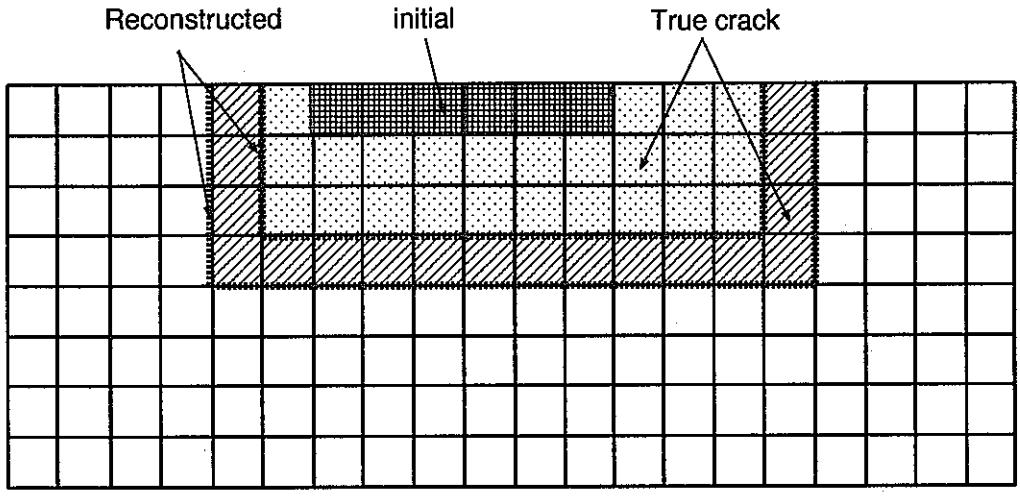

Fig.7 Reconstructed crack shape in case of known conductivity

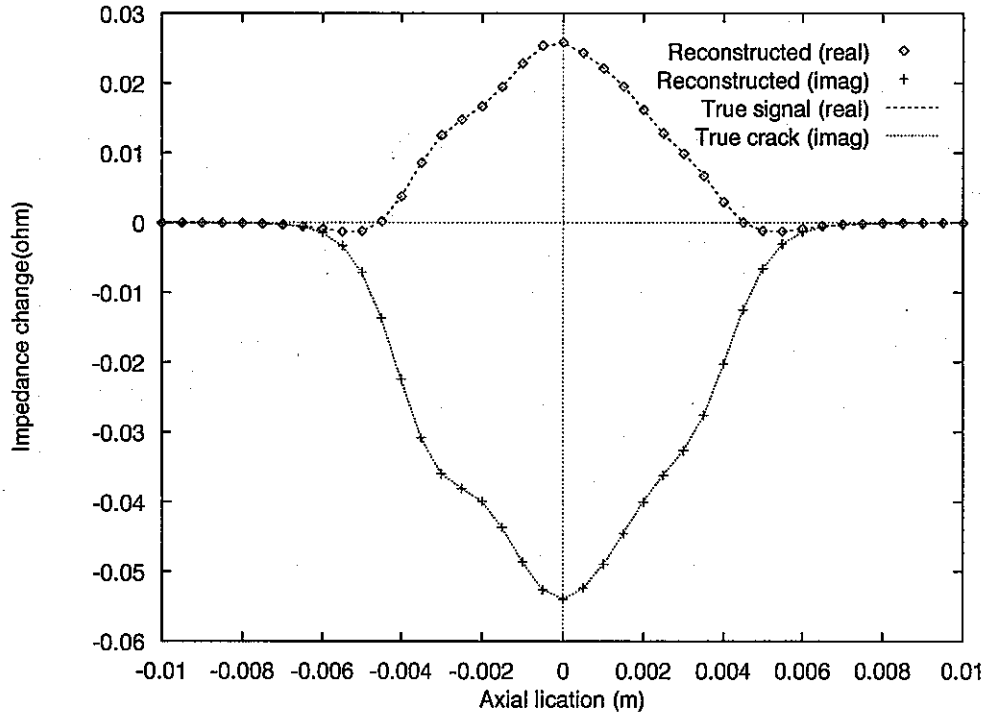

Fig.8 Impedance signals arisen from the reconstructed crack
(with reconstructed conductivity for the conducting band region)

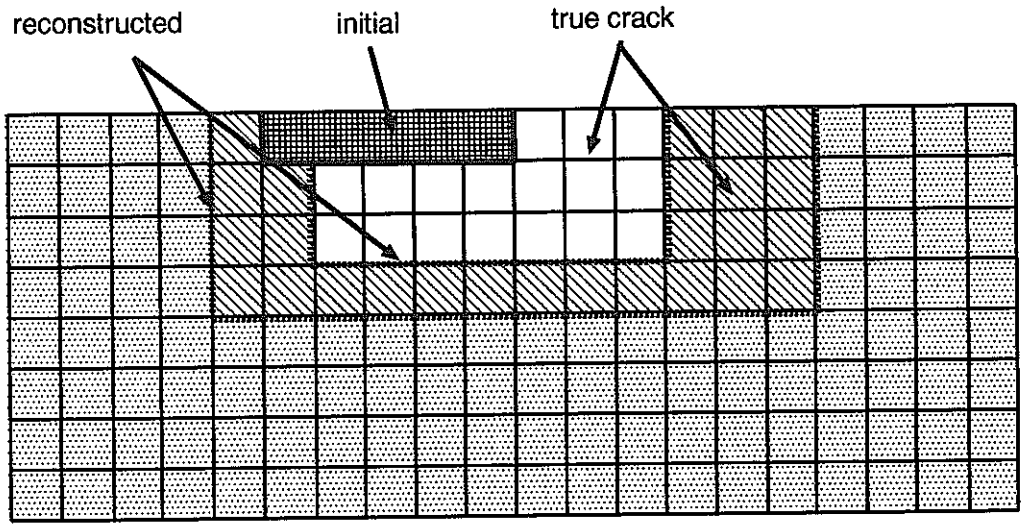

Fig.9 Reconstructed crack shape in case of unknown conductivity

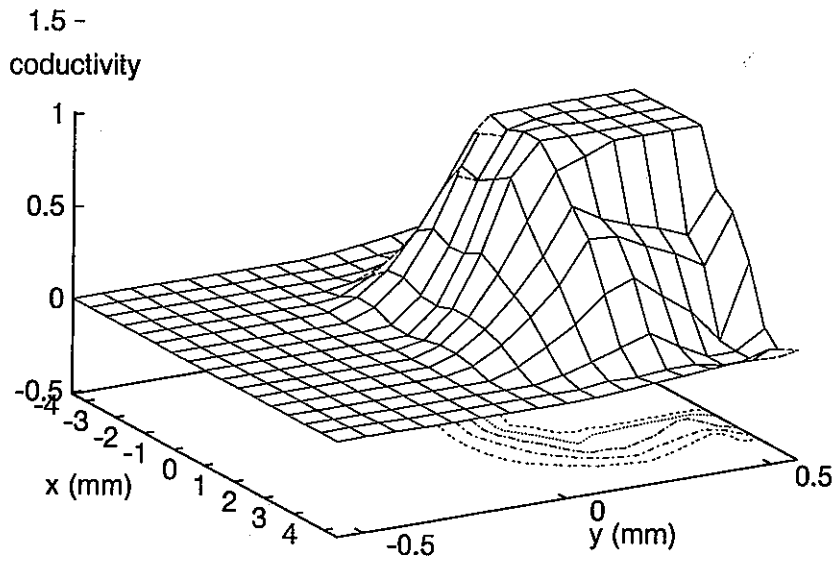

Fig.10 Reconstructed distribution of conductivity

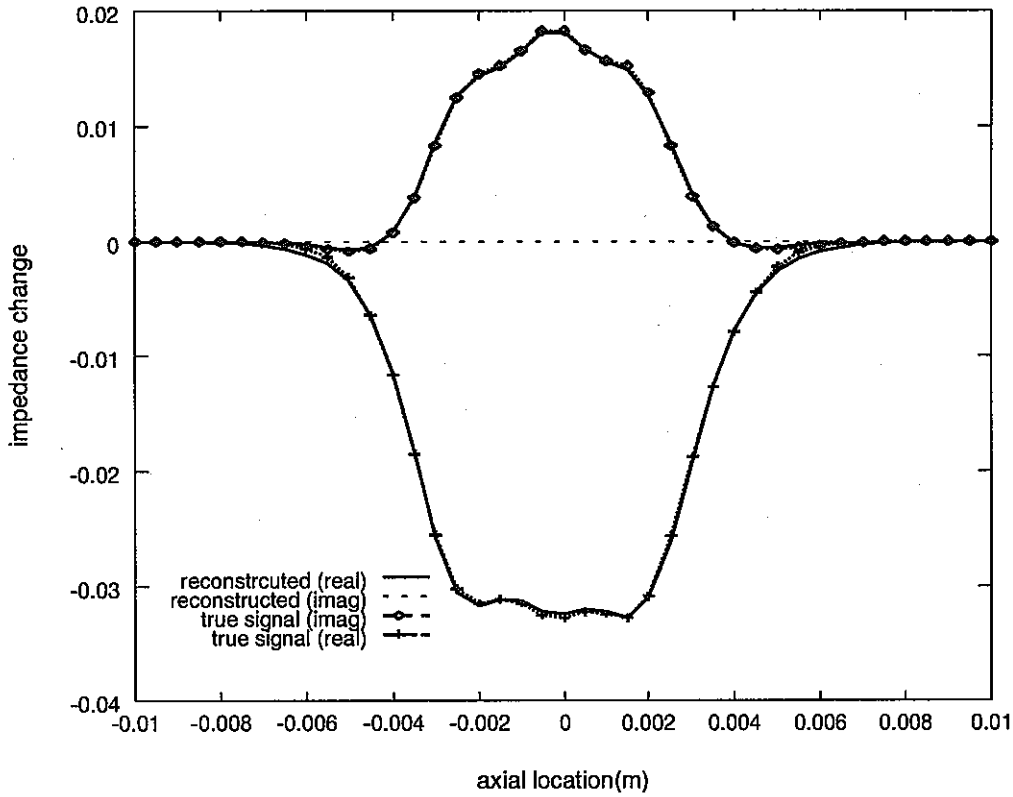

Fig.11 Comparison of impedance signals

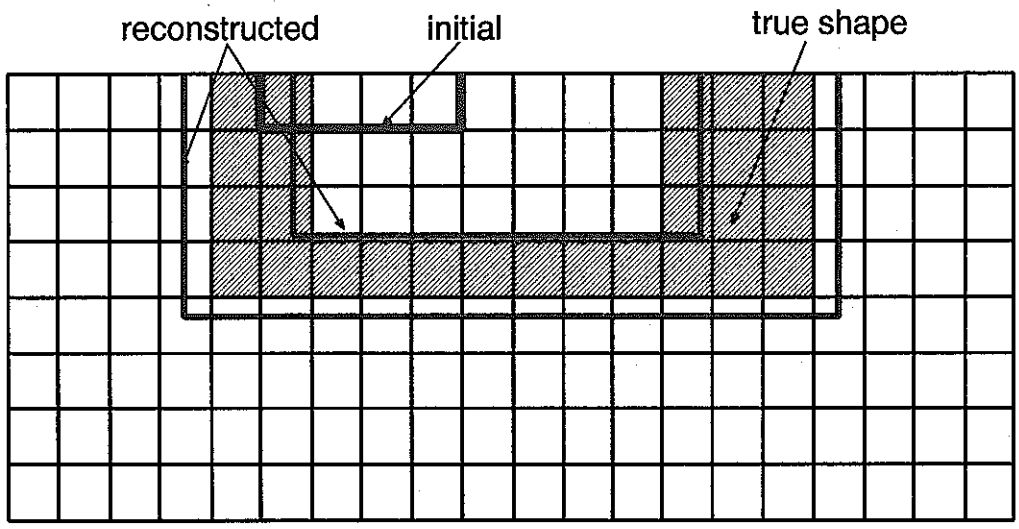

Fig.12 Comparison of the reconstructed crack shape with the true one (5% noise)

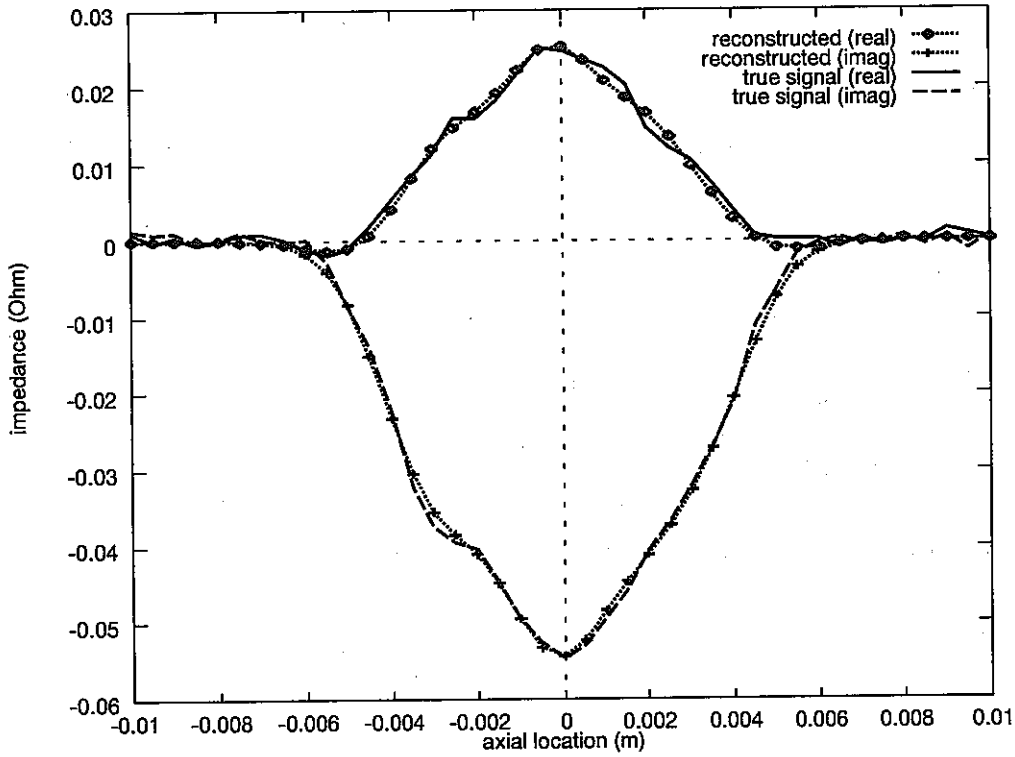

Fig.13 Comparison of impedance signals (5% noise)

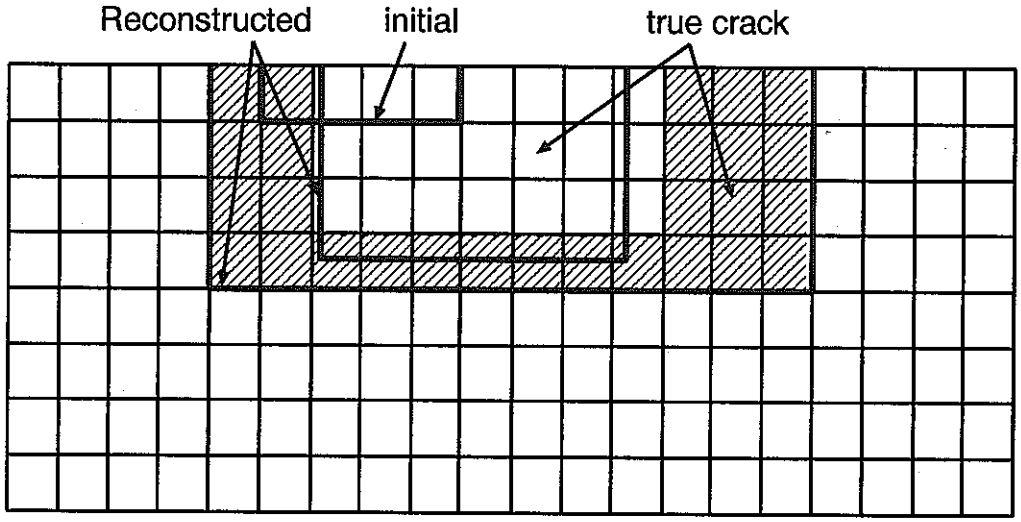

Fig.14 Comparison of the reconstructed crack shape with the true one (10% noise)

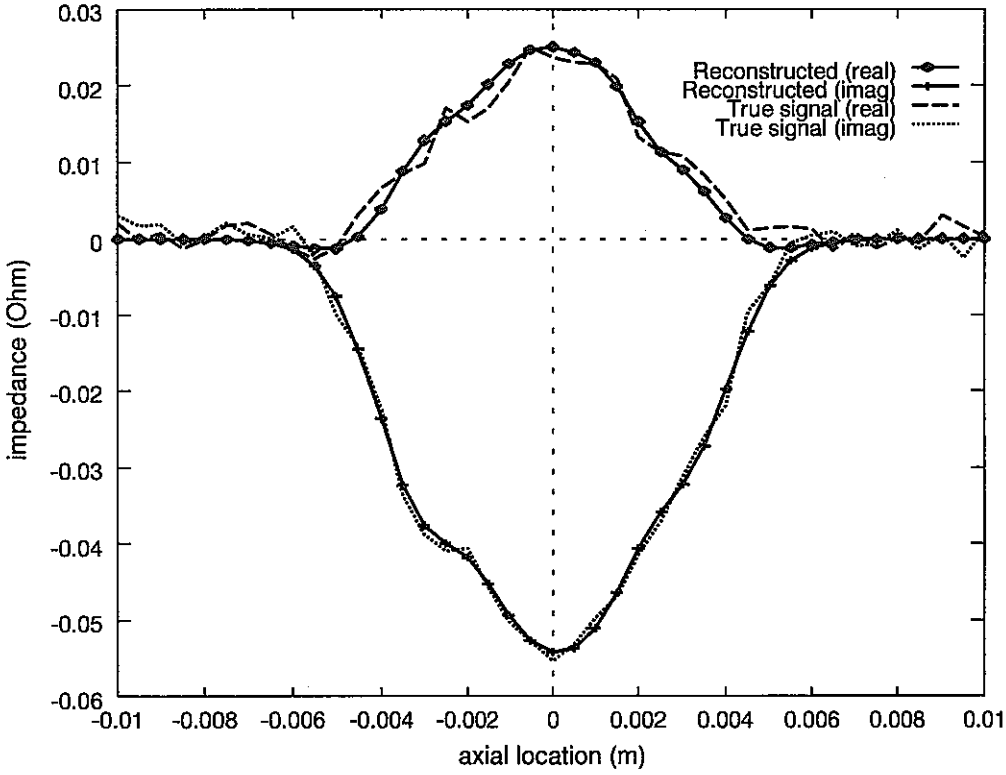

Fig.15 Comparison of impedance signals (10% noise)